BVR$_c$I$_c$ Photometric Observations and Analyses of the Totally Eclipsing, Solar Type Binary, OR Leonis

Ronald G. Samec
Faculty Research Associate, Pisgah Astronomical Research Institute, 1 PARI Drive, Rosman, NC 28772; ronaldsamec@gmail.com

Daniel B. Caton
Dark Sky Observatory, Physics and Astronomy Department, Appalachian State University, 525 Rivers Street, Boone, NC 28608-2106; catondb@appstate.edu

Danny R. Faulkner
Johnson Observatory, 1414 Bur Oak Court, Hebron, KY 41048; dfaulkner@answersingenesis.org

Received May 11, 2019; revised May 28, 2019; accepted May 29, 2019

Abstract CCD, BVR$_c$I$_c$ light curves of OR Leo were taken on 21, 22, 24 January, 11, 25 February, and 11 March 2018 at Dark Sky Observatory in North Carolina with the 0.81-m reflector of Appalachian State University by D. Caton. OR Leo was discovered by the SAVS survey which classified it as a V = 0.51 amplitude, EW variable. Ten times of minimum light were calculated, five primary and five secondary eclipses, from our present observations. The following quadratic ephemeris was determined from all available times of minimum light. The 15-year (~20,000 orbits) period study shows that the orbital period is increasing at a very significant level of confidence: JD Hel Min I = 2458188.65373 (0.00039)d + 0.2709786(0.0000002) × E + 5.6(0.2) × 10^{-10} × E^2. The mass ratio is found to be somewhat extreme, $M_2/M_1 = 0.1827 \pm 0.0004$ ($M_1/M_2 = 5.5$). The total eclipses assure this determination. Its Roche Lobe fill-out is ~24%. The solution had no need of spots. The temperature difference of the components is about ~60 K, with the more massive component the hotter one, so it is an A-type W UMa binary. The inclination is 81.1 ± 0.2°. The secondary eclipse shows a time of constant light with an eclipse duration of 27 minutes.

1. Introduction

In this paper, we continue our analysis of solar type (F-K) eclipsing binaries. These have included all evolutionary configurations, including pre-contact (e.g. Samec *et al.* 2018a), semidetached, Algol (e.g. Caton *et al.* 2017), and V1010 Oph type (e.g. Samec *et al.* 2017a), critical contact (e.g. Samec *et al.* 2017b), overcontact binaries (e.g. Samec *et al.* 2018b), and extreme contact binaries (e.g, Caton *et al.* 2019), which are followed by the violent (Tylenda and Kamiński 2016) red novae stage where the stars coalesce into a single, fast rotating earlier type star. In clusters, these are known as blue stragglers. Here we present the first precision photometry and light curve analysis of another such a binary, the overcontact system OR Leonis.

2. History

CCD photometry at the Star'a Lesn'a Observatory (Pribulla, Vanko, and Hambálek 2009) revealed that two extremely short-period ASAS variables are overcontact binaries. One was J071829-0336.7 (OR Leo), observed during three nights (14 January, 3 February, and 26 March 2009). From the R$_c$ and I$_c$ curves, they estimated a mass ratio, q = 0.15, an inclination, i = 88°, and a fill-out 0.5. The following ephemeris and three times of minimum light were given:

$$\text{JD Hel Min I} = 2454\,905.2867(3) + 0.270969(4)\text{d} \times \text{E}. \quad (1)$$

Their light curves are shown in Figure 1.

VSX gives a magnitude range of R = 13.4–14.0 and the following ephemeris for this binary:

$$\text{HJD Min I} = 2454905.2867 + 0.270969\text{d} \times \text{E}. \quad (2)$$

The system was observed by the All Sky Automated Survey as ASASN-V J113030.89-010156.9 (Pojmański 2002). It gives a Vmax =13.514, an amplitude of 0.39, and an EW (W UMa) designation, J=12.439, K=12.043, B-V=0.552 (E(B-V)= 0.028), and a distance of 195 pc. The ephemeris given is:

$$\text{HJD Min I} = 2457537.80197 + 0.2709608\text{d} \times \text{E}. \quad (3)$$

From the ASAS curves we were able to phase the data with Equation (3) and do parabolic fits to the primary and secondary minima to locate times of "low light" within 0.001 phase of each minimum (see Table 3). Finally, the binary was listed in the 81st Name-List of Variable Stars (Kazarovets *et al.* 2015).

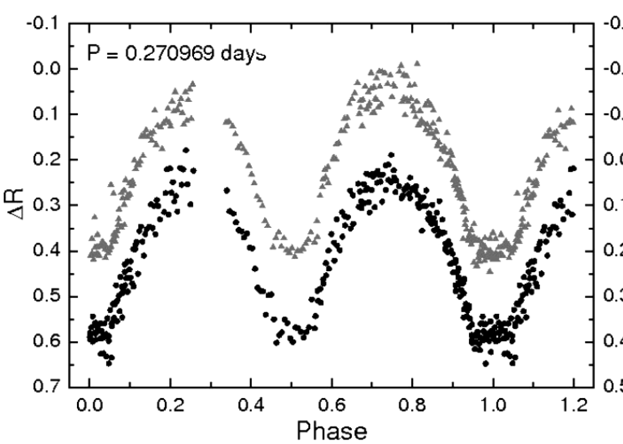

Figure 1. R and I light curves (Pribulla, Vanko, and Hambálek 2009).

Table 1. Information on the stars used in this study.

Star	Name	R.A. (2000) h m s	Dec. (2000)[1] ° ′ ″	V	B–V[2]	J–K[3]
V	OR Leo GSC 04930-00180 2MASS J11303081-0101570 ASAS 113031-0101.9 TYC 04930-00180	11 30 30.8174	–01 01 57.01	13.84	0.55	0.38 ± 0.02[4]
C	GSC 04930-00167	11 30 43.8242	–01 02 49.573	13.74	—	0.38 ± 0.046
K (Check)	GSC 2751-0129 3UC178-119845	11 30 32.1915	–01 05 02.008	14.40	—	0.42 ± 0.0462

[1] *UCAC3 (U.S. Naval Obs. 2012),* [2] *APASS (Henden* et al. *2015),* [3] *2MASS (Skrutskie* et al. *2006),* [4] *spectral type G4.*

3. 2018 BVR_cI_c photometry

The 2018 BVR_cI_c light curves were taken with the Dark Sky Observatory (DSO) 0.81-m reflector at Philips Gap, North Carolina, on 21, 22, 24 January, 11, 25 February, and 11 March 2018 with a thermoelectrically-cooled (–35° C) 2K × 2K Apogee Alta camera and Johnson-Cousins BVR_cI_c filters. The observations were taken by D. Caton. Reduction and analyses were done by R. Samec. This system was observed as a part of our professional collaborative studies of interacting binaries at Pisgah Astronomical Research Institute from data taken from DSO observations. Individual observations included 327 images in B, 325 in V, 338 in R_c, and 337 in I_c. The probable error of a single observation was 9 mmag in B and R_c, 8 mmag in V, and 10 mmag in I_c. The nightly comparison – check star (C–K) values stayed constant throughout the observing run with a precision of 80 mmag in B and R_c and 35 mmag in V and I_c. Exposure times varied from 100s in B, 30–40 s in V, and 20–25 s in R_c and I_c. To produce these images, nightly images were calibrated with 25 bias frames, at least five flat frames in each filter, and ten 300-second dark frames.

The coordinates and magnitudes of the variable star, comparison star, and check star are given in Table 1.

The nightly C–K values stayed constant throughout the observing run with a precision of ≈0.01 mag. Our B–V and R_c–I_c comparison-variable magnitude curves show that the variable and comparison stars are near-spectral matches, with Δ(B–V) and Δ(R_c–I_c) near zero mag.

Figures 2a and 2b show sample observations of B, V, and B–V color curves on the night of 14 September and 15 October 2015.

Our observations are listed in Table 2, with magnitude differences ΔB, ΔV, ΔR_c, and ΔI_c in the sense variable minus comparison star. The finder chart is given in Figure 3 with the variable star (V), comparison star C), and check star (K) shown.

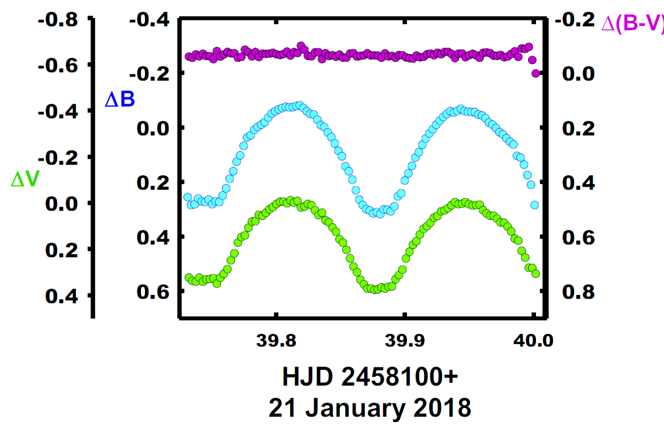

Figure 2a. B, V, and B–V color curves on the night of 21 January 2018.

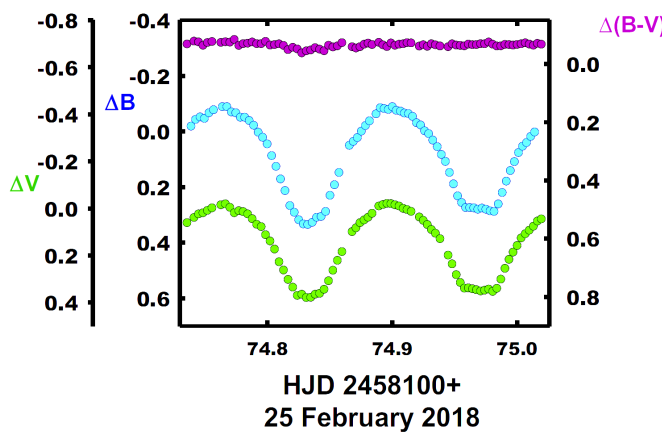

Figure 2b. B, V, and B–V color curves on the night of 25 February 2018.

4. Orbital period study

Ten mean times (from BVR_cI_c data) of minimum light were calculated from our present observations, five primary and five secondary eclipses:

HJD I = 2458139.87973 ± 0.00005, 2458142.8597 ± 0.0005, 2458160.741430 ± 0.000003, 2458174.8331 ± 0.0002, 2458188.6529 ± 0.0012,

HJD II = 2458139.7442 ± 0.0012, 2458142.9903 ± 0.0037, 2458160.8800 ± 0.0008, 2458188.78740 ± 0.0011, 2458174.9709 ± 0.0005.

A least squares minimization method (Mikulášek *et al.* 2014) was used to determine the minima for each curve in B, V, R_c, and I_c. These minima were weighted as 1.0 in the period study. In addition, four times of minimum light were calculated from the data of Pribulla, Vanko, and Hambálek (2009) (weighted 1.0 and a weak timing 0.5). Seven times of "low light" were determined from the ASAS light curve. These are weighted 0.1. A quadratic ephemeris was determined from these data:

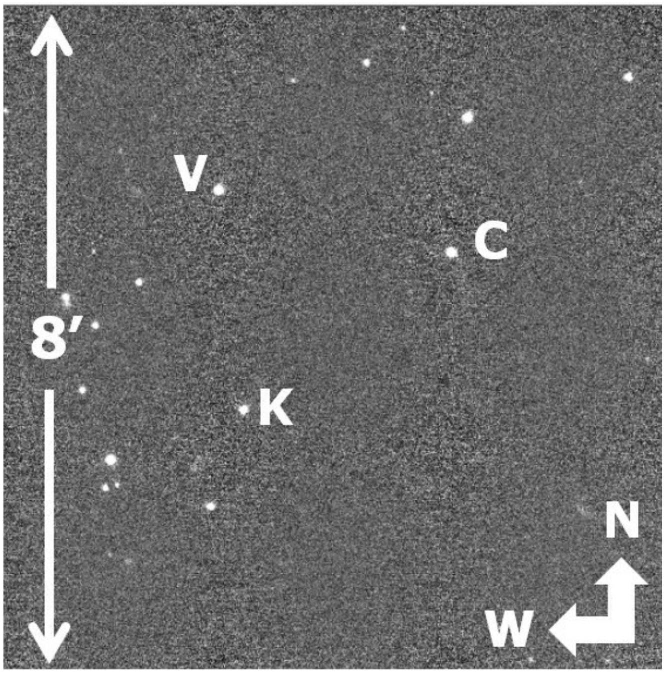

Figure 3. Finder chart, OR Leo (V), Comparison star (C), and check (K).

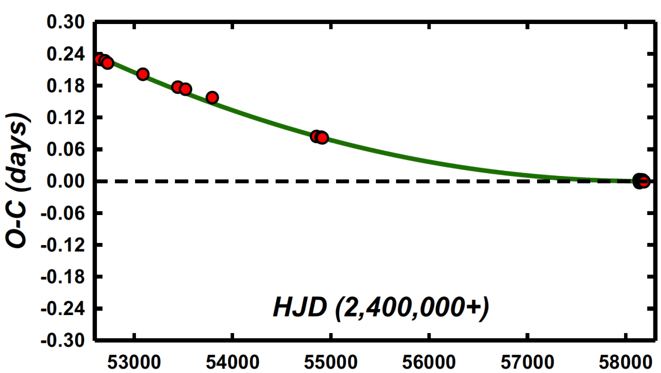

Figure 4. O–C eclipse timing residuals (Equation 3) and quadratic fit of OR Leo from Equation (4).

$$\text{JD Hel Min I} = 2458188.65373 + 0.27097862\text{d} \times \text{E} + 5.6 \times 10^{-10} \quad (4)$$
$$\pm 0.00058 \quad \pm 0.00000031 \qquad \pm 0.2 \times 10^{-10}.$$

A plot of the quadratic residuals is given in Figure 4. The quadratic fit carried a precision of 28 sigma. The O–C quadratic residual calculation results are given in Table 3.

This period study covers a time interval of over 15 years and shows an orbital period that is increasing (at a very significant level of confidence). A possible cause of this effect is mass transfer to the primary component making the mass ratio more extreme. Thus, the primary component is absorbing the secondary component. If this continues, the mass ratio will become more extreme. Ultimately the system would become unstable, resulting in a red novae event and finally a single fast rotating spectrally, earlier star (Tylenda and Kamiński 2016). Alternately, the period change could be a part of a sinusoidal variation due to the presence of a third body.

Using a main sequence mass for the primary, the ephemeris yields a $dP/dt = 1.51 \times 10^{-6}$ d/yr or a mass exchange rate of

$$\frac{dM}{dt} = \frac{\dot{P} M_1 M_2}{3P\,(M_1 - M_2)} = \frac{3.5 \times 10^{-7}\ M_\odot}{\text{d}} \quad (5)$$

in a conservative scenario (the primary component is the gainer).

5. Light curves and temperature determination

The light curve characteristics of OR Leo are given in Table 4. The B, V, R_c, and I_c curves are shown in Figures 5a and 5b. The curves are of fair precision, averaging slightly above 1% photometric precision. The amplitude of the light curves varies from 0.32 to 0.38 magnitude, I_c to B. The O'Connell effect, an indicator of spot activity, averages less than the noise level, 0.003–0.01 magnitude. But, night-to-night variations and scatter in the light curves demonstrate a high magnetic activity level. The differences in minima are small, 0.005–0.04 magnitude, indicating an overcontact binary in fair thermal contact. A time of constant light occurs at our secondary minima and lasts some 27 minutes due to a total eclipse. The 2MASS, $J–K = 0.38 \pm 0.02$ for the binary, and the APASS $(B–V) – E(B–V) = 0.52$. These correspond to ~G4V ± 2.5 spectral type which yields a temperature of 5750 ± 400 K. Fast rotating binary stars of this type are noted for having convective atmospheres, so the binary is of solar type with a convective atmosphere.

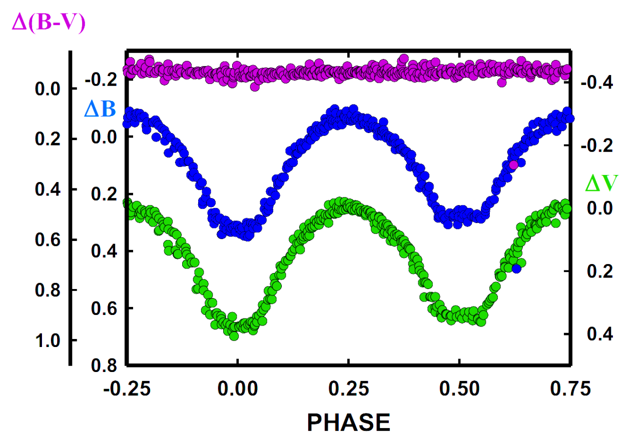

Figure 5a. 2018 B,V light curves and B–V color curves (Variable-Comparison, magnitudes phased with Equation 4.

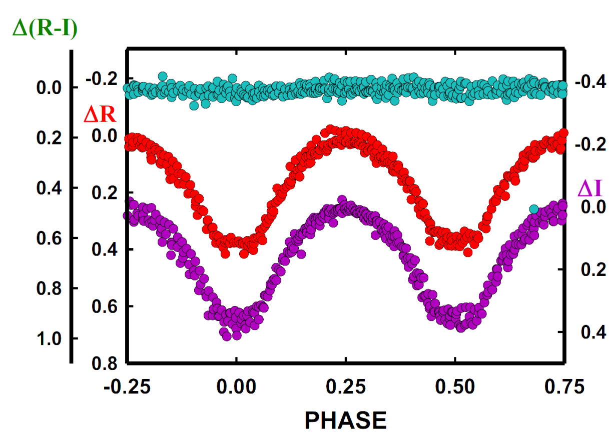

Figure 5b. 2018 R_c,I_c light curves and R_c–I_c color curves (Variable-Comparison, magnitudes phased with Equation 4.

6. Light curve solution

The B, V, R_c, and I_c curves were pre-modeled with BINARY MAKER 3.0 (Bradstreet and Steelman 2002) and fits were determined in BVR_cI_c filter bands which were very stable. The solution was that of an overcontact eclipsing binary. The parameters were then averaged and input into a four-color simultaneous light curve calculation using the Wilson-Devinney program (Wilson and Devinney 1971; Wilson 1990, 1994; Van Hamme and Wilson 1998). The BINARY MAKER parameters included q (mass ratio) = 0.16 ± 0.2, fill-out = 25%, inclination (i) = 84°, and $T_2 - T_1 = 50 \pm 150$ K. The computation was completed in Mode 3 and converged to a solution. Convective parameters g = 0.32, A = 0.5 were used. An eclipse duration of ~27 minutes was determined for our secondary eclipse (phase 0.5) and the light curve solution. The more massive component is the hotter, making the system an A-type W UMa contact binary. In modeling the B,V,R_c,I_c curves simultaneously, the I_c curve was found to be discordant. So we modeled the B,V,R_c curves simultaneously and the Ic curve separately. We feel that there is physical reason for this, such as asymmetrically-placed circumbinary dust or gas or an IR thin disk affecting the I_c curves much more than the visual ones. Our CCD is back-illuminated so red noise could affect the results, but this has not been seen previously on many dozens of cool binaries. We tried third light but that did not solve any fitting issues. More observations are needed to sort this out. Only the simultaneous BVR_cI_c results will be commented on here. The solutions are given in Table 5. The B,V,R_c,I_c normalized fluxes overlaid by our 2018 solution of OR Leo are given as Figures 6a and 6b. Figures 7a–7d display quarter phases of the Roche lobe surface.

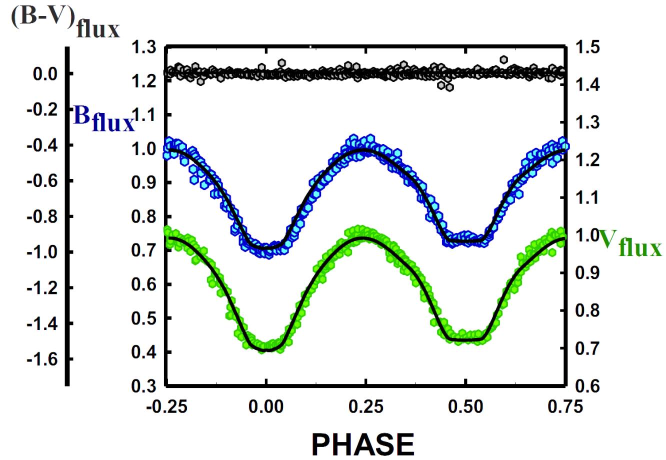

Figure 6a. B, V normalized fluxes and the B–V color curves overlaid by our 2018 solution of OR Leo.

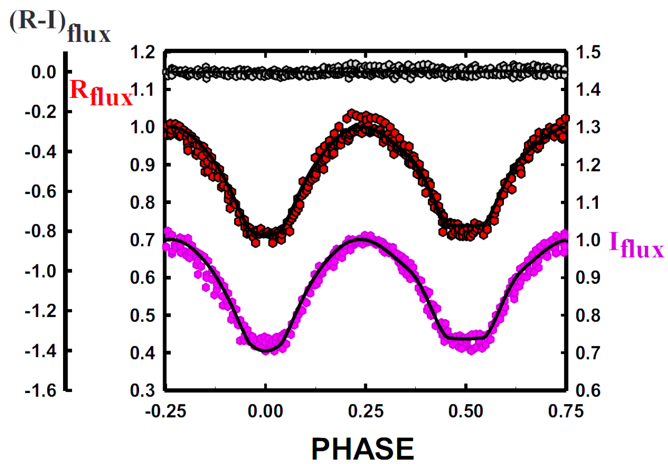

Figure 6b. R_c, I_c normalized fluxes and the R_c–I_c color curves overlaid by our 2018 solution of OR Leo. The I_c curve solution is that shown in Table 5, right hand column.

7. Discussion

OR Leo is an overcontact W UMa binary with a Roche lobe fill-out of 24%. Since the eclipses were total, the mass ratio, q, is well determined. The system has a rather extreme mass ratio of ~0.18 (M_2/M_1), and the component temperature difference is small, only ~60 K. No spots were needed in the modeling. The inclination is ~81 degrees, which results in total eclipses. Its photometric spectral type indicates a surface temperature of ~5750 K for the primary component, making it a solar type binary. Such a main sequence star would have a mass of ~0.92 $M_\odot$ and the secondary (from the mass ratio) would have a mass of ~0.17 $M_\odot$, making it very much undersized for its temperature (~5680 K), but the contact produces a secondary atmosphere with much the same temperature as that of the primary component. Such a main sequence star would be of type M6V. So its true core temperature is completely masked. The W UMa is of A-type, which may mean that it is a mature, very old W UMa binary. However, the fill-out is somewhat low for such a system.

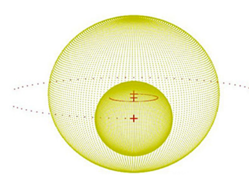

Figure 7a. OR Leo, geometrical representation at phase 0.0.

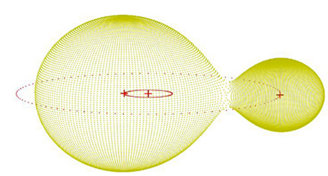

Figure 7b. OR Leo, geometrical representation at phase 0.25.

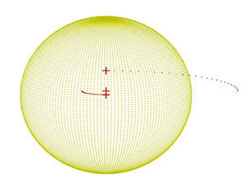

Figure 7c. OR Leo, geometrical representation at phase 0.50.

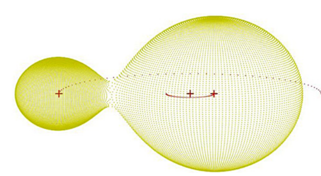

Figure 7d. OR Leo, geometrical representation at phase 0.75.

8. Conclusion

The period study of this overcontact W UMa binary has a 15-year time duration. The period is found to be increasing at about the 27 sigma level. This can happen due to mass transfer to the primary component. We would expect this magnetic braking due to the solar type of the system. If this is occurring, it is moderating the changing of the period, thus making the mass transfer rate actually higher. The mass exchange, if continuous, has decreased the mass of the secondary star, making the mass ratio rather extreme. We would expect that this will eventually cause the system to coalesce following a red novae event (Tylenda and Kamiński 2016). After some system mass loss, one would theorize that the binary will become a rather normal, fast rotating, single ~G0V type field star. As stated in section 4, the observed period increase could be a part of a light-time effect caused by an additional and undetected third body in the system. Finally, radial velocity curves are needed to obtain absolute (not relative) system parameters. More photometric monitoring is needed to determine the nature of the I_c observations. Deeper IR observations could help resolve this problem of the discordant I_c curve.

9. Acknowledgements

Dr. Samec wishes to thank Dr. Bob Hill for his continued observing help and kind friendship through the years.

References

Bradstreet, D. H., and Steelman, D. P. 2002, *Bull. Amer. Astron. Soc*, **34**, 1224.

Caton, D., Gentry, D. R., Samec, R. G., Chamberlain, H., Robb, R., Faulkner, D. R., and Hill, R. 2019, *Publ. Astron. Soc. Pacific*, **131**, 4203.

Caton, D. B., Samec, R. G., Robb, R., Faulkner, D. R., van Hamme, W., Clark, J. D., and Shebs, T. 2017, *Publ. Astron. Soc. Pacific*, **129**, 4202.

Henden, A. A., *et al.* 2015, AAVSO Photometric All-Sky Survey, data release 9 (http://www.aavso.org/apass).

Kazarovets, E. V., Samus, N. N., Durlevich, O. V. Kireeva, N. N., and Pastukhova, E. N. 2015, *Inf. Bull. Var. Stars*, No. 6151, 1.

Mikulášek, Z., Chrastina, M., Liška, J., Zejda, M., Janík, J., Zhu, L.-Y., and Qian, S.-B. 2014, *Contrib. Astron. Obs. Skalnaté Pleso*, **43**, 382.

Pojmański, G. 2002, *Acta Astron.*, **52**, 397.

Pribulla, T., Vanko, M., and Hambalek, L. 2009, *Inf. Bull. Var. Stars*, No. 5886, 1.

Samec, R. G., Caton, D. B., and Faulkner, D. R. 2018a, *J. Amer. Assoc. Var. Star Obs.*, **46**, 57.

Samec, R. G., Caton, D. B., Faulkner, D. R., and Hill, R. 2018b, *J. Amer. Assoc. Var. Star Obs.*, **46**, 106.

Samec, R. G., Norris, C. L., Hill, B. L., van Hamme, W., and Faulkner, D. R. 2017a, *J. Amer. Assoc. Var. Star Obs.*, **45**, 3.

Samec, R. G., Olsen, A., Caton, D. B., Faulkner, D. R., and Hill, R. L. 2017b, *J. Amer. Assoc. Var. Star Obs.*, **45**, 173.

Skrutskie, M. F., *et al.* 2006, *Astron. J.*, **131**, 1163.

Tylenda, R., and Kamiński, T. 2016, *Astron. Astrophys.*, **592A**, 134.

U.S. Naval Observatory. 2012, UCAC-3 (http://www.usno.navy.mil/USNO/astrometry/optical-IR-prod/ucac).

van Hamme, W. V., and Wilson, R. E. 1998, *Bull. Amer. Astron. Soc.*, **30**, 1402.

Wilson, R. E. 1990, *Astrophys. J.*, **356**, 613.

Wilson, R. E. 1994, *Publ. Astron. Soc. Pacific*, **106**, 921.

Wilson, R. E., and Devinney, E. J. 1971, *Astrophys. J.*, **166**, 605.

Table 2. OR Leo observations, ΔB, ΔV, $ΔR_c$, and $ΔI_c$, variable star minus comparison star.

ΔB	BHJD 2458100+	ΔB	BHJD 2458100+	ΔB	BHJD 2458100+	ΔB	BHJD 2458100+	ΔB	BHJD 2458100+
0.257	39.7316	0.042	39.9165	0.161	42.8849	0.163	60.9020	0.277	74.9721
0.286	39.7343	0.023	39.9193	0.143	42.8876	0.112	60.9092	0.281	74.9753
0.283	39.7371	0.008	39.9220	0.107	42.8903	–0.018	74.7390	0.287	74.9786
0.262	39.7398	–0.009	39.9247	0.091	42.8931	–0.042	74.7426	0.289	74.9818
0.273	39.7425	–0.024	39.9274	0.060	42.8958	–0.051	74.7462	0.262	74.9851
0.275	39.7452	–0.037	39.9301	0.041	42.8985	–0.046	74.7498	0.221	74.9883
0.266	39.7479	–0.048	39.9329	0.033	42.9012	–0.066	74.7534	0.180	74.9916
0.283	39.7507	–0.058	39.9356	0.013	42.9039	–0.077	74.7570	0.142	74.9948
0.272	39.7534	–0.053	39.9383	0.001	42.9066	–0.088	74.7641	0.110	74.9981
0.275	39.7561	–0.059	39.9410	–0.025	42.9094	–0.088	74.7677	0.077	75.0014
0.251	39.7588	–0.067	39.9438	–0.030	42.9121	–0.069	74.7713	0.054	75.0046
0.225	39.7615	–0.059	39.9465	–0.036	42.9148	–0.066	74.7749	0.041	75.0078
0.190	39.7642	–0.056	39.9492	–0.055	42.9175	–0.050	74.7785	0.019	75.0111
0.162	39.7670	–0.055	39.9519	–0.038	42.9202	–0.050	74.7820	0.003	75.0143
0.127	39.7697	–0.055	39.9546	–0.041	42.9229	–0.038	74.7856	–0.008	75.0176
0.104	39.7724	–0.046	39.9574	–0.061	42.9257	–0.021	74.7892	–0.045	88.5686
0.069	39.7751	–0.042	39.9601	–0.058	42.9284	0.004	74.7928	–0.053	88.5744
0.038	39.7778	–0.032	39.9628	–0.065	42.9311	0.022	74.7964	–0.034	88.5801
0.030	39.7806	–0.016	39.9655	–0.043	42.9365	0.046	74.8000	–0.043	88.5859
0.010	39.7833	–0.009	39.9683	–0.038	42.9393	0.088	74.8036	–0.075	88.5917
–0.001	39.7860	0.004	39.9710	–0.034	42.9420	0.127	74.8071	–0.057	88.6032
–0.009	39.7887	0.019	39.9737	–0.002	42.9447	0.172	74.8107	0.016	88.6090
–0.018	39.7914	0.027	39.9764	–0.019	42.9474	0.214	74.8143	0.042	88.6147
–0.035	39.7942	0.041	39.9792	0.006	42.9501	0.268	74.8182	0.090	88.6205
–0.050	39.7969	0.054	39.9819	0.019	42.9528	0.292	74.8217	0.142	88.6262
–0.058	39.7996	0.064	39.9846	0.025	42.9556	0.319	74.8253	0.238	88.6320
–0.065	39.8023	0.106	39.9873	0.046	42.9583	0.334	74.8289	0.288	88.6378
–0.070	39.8050	0.112	39.9901	0.057	42.9610	0.336	74.8325	0.321	88.6493
–0.074	39.8078	0.138	39.9928	0.074	42.9637	0.328	74.8361	0.342	88.6551
–0.072	39.8105	0.176	39.9955	0.106	42.9664	0.310	74.8396	0.296	88.6666
–0.073	39.8132	0.212	39.9982	0.128	42.9692	0.307	74.8432	0.259	88.6723
–0.077	39.8159	0.286	40.0010	0.169	42.9719	0.289	74.8468	0.163	88.6781
–0.080	39.8186	0.046	40.7307	0.184	42.9746	0.231	74.8503	0.100	88.6839
–0.070	39.8214	0.024	40.7334	0.217	42.9773	0.193	74.8539	0.060	88.6896
–0.048	39.8268	0.011	40.7361	0.245	42.9800	0.149	74.8575	0.031	88.6954
–0.046	39.8295	0.001	40.7388	0.281	42.9827	0.051	74.8658	–0.030	88.7011
–0.027	39.8323	–0.014	40.7415	0.292	42.9855	0.037	74.8690	–0.049	88.7069
–0.007	39.8350	–0.018	40.7443	0.268	42.9882	0.023	74.8723	–0.096	88.7127
0.020	39.8404	–0.041	40.7470	0.277	42.9909	–0.020	74.8788	–0.070	88.7184
0.037	39.8431	–0.042	40.7497	0.257	42.9936	–0.037	74.8820	–0.096	88.7242
0.060	39.8458	–0.048	40.7524	0.256	42.9963	–0.062	74.8873	–0.061	88.7300
0.087	39.8486	–0.059	40.7551	0.055	60.6394	–0.084	74.8906	–0.001	88.7415
0.107	39.8513	–0.055	40.7578	0.092	60.6440	–0.081	74.8938	0.004	88.7472
0.144	39.8540	–0.053	40.7605	0.032	60.6472	–0.078	74.8971	0.045	88.7530
0.162	39.8567	–0.060	40.7632	0.015	60.6532	–0.088	74.9003	0.107	88.7588
0.193	39.8594	–0.062	40.7660	–0.023	60.6599	–0.075	74.9035	0.180	88.7645
0.232	39.8622	–0.042	40.7687	–0.018	60.6668	–0.072	74.9068	0.175	88.7703
0.266	39.8649	–0.028	40.7714	–0.062	60.6736	–0.065	74.9100	0.278	88.7761
0.286	39.8676	–0.030	40.7741	–0.048	60.6805	–0.063	74.9132	0.284	88.7996
0.301	39.8703	–0.019	40.7768	–0.037	60.6874	–0.053	74.9165	0.235	88.8054
0.306	39.8730	–0.018	40.7795	0.040	60.6942	–0.030	74.9197	0.159	88.8112
0.317	39.8757	–0.006	40.7822	0.058	60.7011	–0.022	74.9230	0.100	88.8169
0.312	39.8785	0.019	40.7850	0.091	60.7080	–0.001	74.9262	0.052	88.8227
0.319	39.8812	0.046	40.7877	0.135	60.7148	0.009	74.9294	0.011	88.8285
0.302	39.8839	0.024	40.7904	0.227	60.7220	0.032	74.9327	–0.002	88.8342
0.303	39.8866	0.287	42.8459	0.306	60.7289	0.056	74.9363	–0.021	88.8400
0.309	39.8893	0.335	42.8550	0.294	60.7358	0.084	74.9396	–0.042	88.8458
0.291	39.8921	0.311	42.8577	–0.050	60.8324	0.109	74.9428	–0.061	88.8515
0.254	39.8948	0.324	42.8604	0.006	60.8392	0.149	74.9461	–0.066	88.8573
0.243	39.8975	0.323	42.8659	0.052	60.8461	0.190	74.9493	–0.081	88.8630
0.196	39.9002	0.322	42.8686	0.119	60.8529	0.233	74.9526	–0.023	88.8688
0.170	39.9030	0.321	42.8713	0.198	60.8598	0.257	74.9558	0.003	88.8746
0.143	39.9057	0.293	42.8740	0.270	60.8667	0.275	74.9591	0.039	88.8861
0.112	39.9084	0.265	42.8767	0.287	60.8804	0.275	74.9623		
0.092	39.9111	0.228	42.8795	0.283	60.8876	0.276	74.9656		
0.065	39.9138	0.207	42.8822	0.241	60.8948	0.281	74.9688		

Table continued on following pages

Table 2. OR Leo observations, ΔB, ΔV, ΔR_c, and ΔI_c, variable star minus comparison star, cont.

ΔV	VHJD 2458100+	ΔV	VHJD 2458100+	ΔV	VHJD 2458100+	ΔV	VHJD 2458100+	ΔV	VHJD 2458100+
0.325	39.7326	0.114	39.9148	0.214	42.8858	0.025	74.7450	0.341	74.9840
0.339	39.7353	0.102	39.9175	0.168	42.8885	0.020	74.7486	0.302	74.9872
0.342	39.7380	0.087	39.9202	0.153	42.8913	0.010	74.7521	0.256	74.9905
0.325	39.7407	0.065	39.9229	0.130	42.8940	–0.001	74.7558	0.218	74.9938
0.342	39.7434	0.058	39.9256	0.113	42.8967	–0.002	74.7594	0.187	74.9970
0.332	39.7461	0.038	39.9284	0.091	42.8994	–0.014	74.7629	0.159	75.0003
0.331	39.7489	0.034	39.9311	0.075	42.9021	–0.018	74.7665	0.127	75.0035
0.328	39.7516	0.024	39.9338	0.061	42.9049	–0.003	74.7701	0.109	75.0068
0.351	39.7543	0.012	39.9365	0.046	42.9076	0.020	74.7737	0.094	75.0100
0.325	39.7570	–0.002	39.9392	0.019	42.9103	0.011	74.7773	0.077	75.0133
0.308	39.7597	0.007	39.9420	0.022	42.9130	0.015	74.7808	0.055	75.0165
0.288	39.7625	0.005	39.9447	0.019	42.9157	0.025	74.7844	0.046	75.0197
0.250	39.7652	–0.002	39.9474	0.017	42.9184	0.045	74.7880	0.054	88.5641
0.220	39.7679	0.007	39.9501	–0.003	42.9212	0.069	74.7916	0.026	88.5705
0.173	39.7706	0.013	39.9529	–0.003	42.9266	0.079	74.7952	–0.011	88.5763
0.149	39.7733	0.011	39.9556	0.005	42.9293	0.113	74.7987	0.016	88.5821
0.142	39.7761	0.009	39.9583	0.001	42.9320	0.140	74.8023	0.025	88.5878
0.109	39.7788	0.033	39.9610	0.010	42.9347	0.174	74.8059	0.033	88.5936
0.082	39.7815	0.047	39.9637	0.014	42.9375	0.228	74.8095	0.025	88.5994
0.081	39.7842	0.057	39.9665	0.019	42.9402	0.263	74.8131	0.074	88.6051
0.053	39.7869	0.057	39.9692	0.027	42.9429	0.303	74.8167	0.148	88.6167
0.057	39.7897	0.070	39.9719	0.031	42.9456	0.336	74.8205	0.179	88.6224
0.044	39.7924	0.086	39.9746	0.053	42.9483	0.371	74.8241	0.259	88.6282
0.029	39.7951	0.088	39.9774	0.058	42.9511	0.366	74.8277	0.326	88.6339
0.019	39.7978	0.104	39.9801	0.076	42.9538	0.380	74.8313	0.372	88.6397
0.006	39.8005	0.125	39.9828	0.084	42.9565	0.379	74.8349	0.384	88.6570
–0.003	39.8033	0.156	39.9856	0.108	42.9592	0.366	74.8384	0.390	88.6628
–0.004	39.8060	0.165	39.9883	0.116	42.9619	0.362	74.8420	0.360	88.6685
0.003	39.8087	0.209	39.9910	0.132	42.9646	0.345	74.8456	0.291	88.6743
–0.010	39.8114	0.238	39.9937	0.155	42.9674	0.309	74.8491	0.193	88.6801
–0.007	39.8169	0.282	39.9965	0.186	42.9701	0.264	74.8527	0.153	88.6858
0.021	39.8196	0.283	39.9992	0.215	42.9728	0.222	74.8563	0.133	88.6916
0.017	39.8223	0.308	40.0019	0.243	42.9755	0.185	74.8599	0.088	88.6973
0.006	39.8250	0.100	40.7316	0.285	42.9782	0.100	74.8680	0.054	88.7031
0.012	39.8278	0.091	40.7343	0.314	42.9810	0.084	74.8712	0.048	88.7089
0.034	39.8305	0.064	40.7370	0.345	42.9837	0.062	74.8744	0.017	88.7146
0.054	39.8332	0.046	40.7398	0.338	42.9864	0.050	74.8777	–0.009	88.7204
0.044	39.8359	0.039	40.7425	0.345	42.9891	0.039	74.8809	–0.008	88.7262
0.077	39.8386	0.038	40.7452	0.358	43.0027	0.022	74.8841	0.019	88.7319
0.086	39.8413	0.020	40.7479	0.217	60.6337	–0.009	74.8895	0.027	88.7357
0.108	39.8441	0.020	40.7506	0.144	60.6386	–0.015	74.8927	0.068	88.7377
0.127	39.8468	0.004	40.7533	0.167	60.6409	–0.020	74.8960	0.077	88.7434
0.159	39.8495	0.007	40.7560	0.144	60.6433	–0.019	74.8992	0.108	88.7492
0.174	39.8522	–0.001	40.7587	0.062	60.6510	–0.014	74.9024	0.145	88.7550
0.205	39.8549	0.009	40.7615	0.016	60.6642	–0.009	74.9057	0.196	88.7607
0.242	39.8577	0.001	40.7642	0.011	60.6711	0.001	74.9089	0.238	88.7665
0.277	39.8604	0.013	40.7669	0.007	60.6780	0.006	74.9121	0.321	88.7722
0.302	39.8631	0.025	40.7696	0.006	60.6849	0.014	74.9154	0.349	88.7780
0.334	39.8658	0.015	40.7723	0.046	60.6917	0.038	74.9219	0.358	88.7838
0.354	39.8685	0.051	40.7750	0.062	60.6986	0.052	74.9251	0.296	88.8074
0.373	39.8712	0.028	40.7778	0.135	60.7055	0.070	74.9283	0.208	88.8131
0.372	39.8740	0.083	40.7805	0.149	60.7123	0.091	74.9316	0.125	88.8246
0.378	39.8767	0.082	40.7832	0.257	60.7192	0.107	74.9348	0.084	88.8304
0.376	39.8794	0.095	40.7859	0.340	60.7264	0.130	74.9385	0.066	88.8362
0.367	39.8821	0.102	40.7913	0.344	60.7332	0.200	74.9450	0.045	88.8419
0.372	39.8849	0.344	42.8469	0.392	60.7401	0.237	74.9482	0.049	88.8477
0.364	39.8876	0.364	42.8505	0.372	60.7538	0.283	74.9515	0.022	88.8534
0.363	39.8903	0.375	42.8614	0.105	60.8367	0.316	74.9547	0.014	88.8592
0.332	39.8930	0.382	42.8641	0.127	60.8436	0.340	74.9580	0.012	88.8650
0.314	39.8957	0.370	42.8668	0.178	60.8504	0.339	74.9612	0.036	88.8707
0.290	39.8984	0.376	42.8695	0.284	60.8573	0.343	74.9645	0.071	88.8765
0.242	39.9012	0.343	42.8722	0.332	60.8642	0.347	74.9677		
0.213	39.9039	0.324	42.8750	0.285	60.8993	0.352	74.9710		
0.183	39.9066	0.292	42.8777	0.190	60.9066	0.349	74.9742		
0.167	39.9093	0.264	42.8804	0.062	74.7358	0.344	74.9775		
0.138	39.9120	0.249	42.8831	0.040	74.7414	0.354	74.9807		

Table continued on following pages

Table 2. OR Leo observations, ΔB, ΔV, $ΔR_c$, and $ΔI_c$, variable star minus comparison star, cont.

Δ*R*	*RHJD 2458100+*	Δ*R*	*RHJD 2458100+*	Δ*R*	*RHJD 2458100+*	Δ*R*	*RHJD 2458100+*	Δ*R*	*RHJD 2458100+*
0.139	40.729	0.021	42.922	0.258	60.856	–0.007	74.889	0.097	88.606
0.111	40.732	0.013	42.924	0.334	60.863	–0.021	74.892	0.128	88.612
0.076	40.735	0.024	42.927	0.380	60.870	–0.015	74.895	0.171	88.618
0.096	40.738	0.028	42.930	0.389	60.877	–0.010	74.899	0.206	88.624
0.070	40.740	0.025	42.933	0.378	60.884	–0.015	74.902	0.281	88.629
0.052	40.743	0.034	42.935	0.383	60.891	–0.008	74.905	0.331	88.635
0.044	40.746	0.041	42.938	0.328	60.898	–0.008	74.908	0.379	88.641
0.040	40.748	0.054	42.941	0.192	60.905	–0.002	74.912	0.417	88.647
0.031	40.751	0.053	42.943	0.071	74.741	0.006	74.915	0.417	88.658
0.029	40.754	0.057	42.946	0.054	74.744	0.018	74.918	0.404	88.664
0.035	40.757	0.075	42.949	0.034	74.748	0.035	74.921	0.370	88.670
0.025	40.759	0.081	42.952	0.035	74.751	0.050	74.924	0.282	88.675
0.033	40.762	0.093	42.954	0.019	74.755	0.072	74.928	0.218	88.681
0.027	40.765	0.108	42.957	0.021	74.759	0.075	74.931	0.174	88.687
0.027	40.767	0.116	42.960	0.004	74.762	0.106	74.934	0.146	88.693
0.037	40.770	0.140	42.962	–0.008	74.766	0.131	74.938	0.100	88.698
0.054	40.773	0.161	42.965	0.008	74.769	0.162	74.941	0.069	88.704
0.050	40.776	0.190	42.968	0.022	74.773	0.189	74.944	0.050	88.710
0.098	40.778	0.199	42.971	0.042	74.777	0.233	74.948	0.026	88.716
0.076	40.781	0.248	42.973	0.044	74.780	0.274	74.951	–0.003	88.722
0.102	40.786	0.288	42.976	0.052	74.784	0.311	74.954	0.023	88.727
0.129	40.789	0.307	42.979	0.070	74.787	0.340	74.957	0.062	88.733
0.325	42.845	0.341	42.981	0.104	74.791	0.350	74.961	0.078	88.739
0.357	42.848	0.336	42.984	0.122	74.794	0.342	74.964	0.125	88.750
0.394	42.851	0.341	42.987	0.135	74.798	0.358	74.967	0.162	88.756
0.369	42.854	0.368	42.990	0.162	74.802	0.356	74.970	0.226	88.762
0.382	42.862	0.377	42.992	0.201	74.805	0.359	74.974	0.279	88.768
0.385	42.865	0.389	42.995	0.232	74.809	0.358	74.977	0.372	88.773
0.377	42.867	0.391	42.998	0.262	74.812	0.368	74.980	0.386	88.779
0.381	42.870	0.338	43.001	0.301	74.816	0.352	74.983	0.388	88.785
0.359	42.873	0.143	60.640	0.353	74.820	0.320	74.987	0.384	88.791
0.329	42.875	0.143	60.643	0.381	74.823	0.284	74.990	0.358	88.803
0.308	42.878	0.161	60.645	0.377	74.827	0.235	74.993	0.300	88.808
0.267	42.881	0.112	60.650	0.360	74.831	0.208	74.996	0.225	88.814
0.236	42.884	0.081	60.656	0.377	74.834	0.171	75.000	0.214	88.820
0.207	42.886	0.032	60.663	0.378	74.838	0.147	75.003	0.146	88.826
0.187	42.889	0.035	60.670	0.389	74.841	0.124	75.006	0.108	88.832
0.164	42.892	0.041	60.677	0.362	74.845	0.105	75.009	0.079	88.837
0.142	42.895	0.037	60.684	0.334	74.848	0.089	75.013	0.039	88.843
0.122	42.897	0.079	60.691	0.294	74.852	0.072	75.016	0.045	88.849
0.112	42.900	0.091	60.697	0.246	74.856	0.073	75.019	0.046	88.855
0.077	42.903	0.153	60.704	0.187	74.859	0.074	88.566	0.036	88.860
0.070	42.905	0.173	60.711	0.110	74.867	0.051	88.572	0.044	88.866
0.063	42.908	0.249	60.718	0.088	74.871	0.031	88.577	0.087	88.872
0.052	42.911	0.399	60.753	0.074	74.874	0.052	88.583	0.101	88.878
0.035	42.914	0.092	60.836	0.058	74.877	0.041	88.589	0.155	88.883
0.033	42.916	0.129	60.842	0.037	74.880	0.029	88.595		
0.030	42.919	0.188	60.849	0.016	74.884	0.063	88.601		

Table continued on next page

Table 2. OR Leo observations, ΔB, ΔV, ΔR_c, and ΔI_c, variable star minus comparison star, cont.

ΔI	IHJD 2458100+	ΔI	IHJD 2458100+	ΔI	IHJD 2458100+	ΔI	IHJD 2458100+	ΔI	IHJD 2458100+
0.111	40.730	0.022	42.925	0.253	60.855	0.020	74.888	0.071	88.607
0.088	40.733	0.006	42.928	0.309	60.862	0.018	74.892	0.156	88.613
0.076	40.735	–0.003	42.930	0.334	60.869	0.019	74.895	0.181	88.619
0.074	40.738	0.019	42.933	0.350	60.876	0.007	74.898	0.217	88.624
0.044	40.741	0.019	42.936	0.388	60.883	0.009	74.901	0.268	88.630
0.039	40.743	0.016	42.938	0.378	60.890	0.014	74.905	0.348	88.636
0.039	40.746	0.035	42.941	0.307	60.897	0.016	74.908	0.390	88.653
0.028	40.749	0.036	42.944	0.241	60.904	0.018	74.911	0.379	88.659
0.008	40.754	0.058	42.947	0.195	60.912	0.023	74.914	0.380	88.665
0.013	40.760	0.075	42.949	0.090	74.740	0.048	74.917	0.324	88.671
0.009	40.762	0.068	42.952	0.052	74.744	0.047	74.921	0.234	88.676
0.013	40.765	0.094	42.955	0.061	74.747	0.074	74.924	0.172	88.682
0.011	40.768	0.097	42.957	0.052	74.751	0.076	74.927	0.146	88.688
0.039	40.771	0.115	42.960	0.017	74.754	0.108	74.930	0.090	88.699
0.037	40.773	0.132	42.963	0.020	74.758	0.116	74.934	0.062	88.705
0.044	40.776	0.165	42.966	0.014	74.762	0.157	74.937	0.039	88.711
0.047	40.779	0.183	42.968	–0.001	74.765	0.194	74.941	0.010	88.717
0.073	40.781	0.213	42.971	–0.004	74.769	0.224	74.944	0.016	88.722
0.103	40.784	0.228	42.974	0.023	74.772	0.250	74.947	0.023	88.728
0.115	40.787	0.286	42.976	0.037	74.776	0.285	74.950	0.046	88.734
0.079	40.790	0.319	42.979	0.044	74.780	0.326	74.954	0.093	88.745
0.328	42.845	0.333	42.982	0.044	74.783	0.337	74.957	0.128	88.751
0.350	42.849	0.337	42.985	0.060	74.787	0.350	74.960	0.159	88.757
0.366	42.854	0.337	42.987	0.089	74.790	0.361	74.963	0.234	88.763
0.376	42.857	0.374	42.990	0.116	74.794	0.379	74.967	0.291	88.769
0.373	42.862	0.337	42.993	0.130	74.797	0.358	74.970	0.351	88.774
0.390	42.865	0.344	42.995	0.146	74.801	0.383	74.973	0.363	88.780
0.370	42.868	0.388	42.998	0.186	74.805	0.374	74.976	0.359	88.786
0.340	42.870	0.378	43.001	0.221	74.808	0.371	74.980	0.379	88.792
0.361	42.873	0.157	60.638	0.249	74.812	0.365	74.983	0.352	88.798
0.321	42.876	0.179	60.640	0.288	74.815	0.343	74.986	0.341	88.804
0.288	42.879	0.154	60.642	0.348	74.819	0.283	74.989	0.274	88.809
0.250	42.881	0.138	60.645	0.351	74.823	0.266	74.993	0.201	88.815
0.236	42.884	0.122	60.649	0.369	74.826	0.224	74.996	0.156	88.821
0.208	42.887	0.086	60.655	0.340	74.830	0.173	74.999	0.120	88.827
0.175	42.889	0.045	60.662	0.355	74.834	0.174	75.002	0.105	88.832
0.149	42.892	0.048	60.669	0.360	74.837	0.152	75.006	0.050	88.838
0.134	42.895	0.030	60.676	0.349	74.841	0.122	75.009	0.059	88.844
0.104	42.898	0.030	60.683	0.339	74.844	0.109	75.012	0.048	88.850
0.090	42.900	0.055	60.690	0.321	74.848	0.107	75.015	0.028	88.856
0.083	42.903	0.084	60.697	0.284	74.851	0.093	75.019	0.043	88.861
0.046	42.906	0.124	60.703	0.249	74.855	0.071	88.567	0.047	88.867
0.056	42.909	0.164	60.710	0.196	74.859	0.053	88.573	0.063	88.873
0.046	42.911	0.205	60.717	0.114	74.867	0.034	88.578	0.114	88.879
0.026	42.914	0.277	60.724	0.088	74.870	0.046	88.584	0.115	88.884
0.013	42.917	0.307	60.731	0.095	74.873	0.050	88.590		
0.023	42.919	0.081	60.835	0.073	74.877	0.027	88.596		
0.016	42.922	0.172	60.848	0.052	74.880	0.048	88.601		

Table 3. O–C residuals for OR Leo.

	Epoch 2400000+	Cycles	Linear Residuals	Quadratic Residuals	Weight	Reference
1	52652.7891	–20430.0	0.0637	–0.0048	0.1	ASAS (Pojmański 2002)
2	52706.7113	–20231.0	0.0628	–0.0028	0.1	ASAS (Pojmański 2002)
3	52733.8048	–20131.0	0.0593	–0.0049	0.1	ASAS (Pojmański 2002)
4	53092.6950	–18806.5	0.0492	0.0030	0.1	ASAS (Pojmański 2002)
5	53446.7043	–17500.0	0.0356	0.0052	0.1	ASAS (Pojmański 2002)
6	53525.5551	–17209.0	0.0340	0.0069	0.1	ASAS (Pojmański 2002)
7	53797.7374	–16204.5	0.0265	0.0099	0.1	ASAS (Pojmański 2002)
8	54857.5970	–12293.0	–0.0147	–0.0010	0.5	Pribulla *et al.* (2009)
9	54905.4228	–12116.5	–0.0151	–0.0005	1.0	Pribulla *et al.* (2009)
10	54905.5589	–12116.0	–0.0145	0.0001	1.0	Pribulla *et al.* (2009)
11	54917.4808	–12072.0	–0.0153	–0.0005	1.0	Pribulla *et al.* (2009)
12	58139.7442	–180.5	0.0033	0.0021	1.0	Present observations
13	58139.8797	–180.0	0.0034	0.0021	1.0	Present observations
14	58142.8597	–169.0	0.0027	0.0013	1.0	Present observations
15	58142.9903	–168.5	–0.0022	–0.0036	1.0	Present observations
16	58160.7414	–103.0	0.0003	–0.0015	1.0	Present observations
17	58160.8800	–102.5	0.0035	0.0016	1.0	Present observations
18	58174.8331	–51.0	0.0016	–0.0007	1.0	Present observations
19	58174.9709	–50.5	0.0039	0.0016	1.0	Present observations
20	58188.6529	0.0	0.0019	–0.0008	1.0	Present observations
21	58188.7874	0.5	0.0009	–0.0018	1.0	Present observations

Table 4. Light curve characteristics for OR Leo.

Filter	Phase 0.00	Magnitude* Min. I	Phase 0.25	Magnitude* Max. II
B		0.377 ± 0.008		0.016 ± 0.017
V		0.359 ± 0.020		0.007 ± 0.010
R		0.319 ± 0.017		–0.062 ± 0.011
I		0.359 ± 0.020		0.007 ± 0.010
Filter	*Phase 0.50*	*Magnitude Min. II*	*Phase 0.75*	*Magnitude Max. I*
B		0.365 ± 0.015		0.019 ± 0.013
V		0.354 ± 0.023		0.010 ± 0.003
R		0.275 ± 0.009		–0.072 ± 0.012
I		0.354 ± 0.023		0.010 ± 0.020

Filter	Min. I – Max. II	Max. I – Max. II	Min. I – Min. II
B	0.3607 ± 0.0253	0.0029 ± 0.0305	0.0118 ± 0.0236
V	0.3525 ± 0.0303	0.0029 ± 0.0134	0.0052 ± 0.0429
R	0.3817 ± 0.0282	0.0098 ± 0.0230	0.0440 ± 0.0263
I	0.3525 ± 0.0303	0.0029 ± 0.0299	0.0052 ± 0.0430

*Magnitude is the variable star – comparison star magnitude.

Table 5. B,V,Rc,Ic, solution parameters.

Parameters	B,V, R_c Values	I_c Values
λB, λV, λR,λI (nm)	440, 550, 640	790
$x_{bol1,2}$, $y_{bol1,2}$	0.570, 0.269, 0.570, 0.269	0.570, 0.269, 0.570, 0.269
$x_{1I,2I}$, $y_{1I,2I}$	—	0.839, 0.145, 0.839, 0.145
$x_{1R,2R}$, $y_{1R,2R}$	0.762, 0.232, 0.762, 0.232	—
$x_{1V,2V}$, $y_{1V,2V}$	0.691, 0.251, 0.691, 0.251	—
$x_{1B,2B}$, $y_{1B,2B}$	0.607, 0.246, 0.607, 0.246	—
g_1 , g_2	0.32	0.32
A_1 , A_2	0.5	0.5
Inclination (°)	81.1 ± 0.1	79.3 ± 0.3
T_1, T_2 (K)	5750*, 5683 ± 4	5750*, 5890 ± 12
Epoch	2458188.6529 ± 0.0015	2458188.6523 ± 0.0003
Period	0.270961 ± 0.000001	0.270958 ± 0.000002
$\Omega_1 = \Omega_2$	2.1613 ± 0.0015	2.078 ± 0.003
$q(m_2 / m_1)$*	0.1827 ± 0.0004	0.1505 ± 0.0006
$F_1 = F_2$ (%)	24 ± 1	28 ± 1
$L_1 / (L_1 + L_2)_I$	—	0.832 ± 0.009
$L_1 / (L_1 + L_2)_R$	0.826 ± 0.007	—
$L_1 / (L_1 + L_2)_V$	0.827 ± 0.010	—
$L_1 / (L_1 + L_2)_B$	0.829 ± 0.009	—

*±400 K.